Sputtering yields of Si, SiC, and B_4C under nanodroplet bombardment at normal incidence

Manuel Gamero-Castaño[a] and Mahesh Mahadevan
Department of Mechanical and Aerospace Engineering, University of California, Irvine, California 92697, USA

(Received 30 May 2009; accepted 20 July 2009; published online 3 September 2009)

Single-crystal silicon and polycrystalline silicon carbide and boron carbide were bombarded with a beam of electrosprayed nanodroplets at normal incidence. The acceleration voltage of the beam ranged between 9.13 and 20.13 kV. The kinetic energy of the nanodroplet molecules varied between 24.1 and 91.2 eV. The volume of sputtered material was measured with a profilometer, and the molecular flux of the beamlet with a time of flight spectrometer. Sputtering yields as high as 2.32, 1.48, and 2.29 atoms per molecule were obtained for Si, SiC, and B_4C. The maximum receding rates of the substrates' surfaces were 448, 172, and 170 nm/min respectively. The significant increase with respect to the sputtering rates of broad-beam atomic ion sources is due to the large molecular flux of electrosprays. © *2009 American Institute of Physics*. [doi:10.1063/1.3211304]

I. INTRODUCTION

We have recently shown that electrosprayed nanodroplets accelerated in a vacuum by a potential difference of the order of ten kilovolts, and impacting on a Si wafer, release a number of Si atoms comparable to the number of molecules in the droplet.[1] The phenomenology of nanodroplet sputtering is likely similar to that of cluster ion beams, a major difference being the method used to produce the projectiles: electrohydrodynamic atomization of a liquid in the case of charged nanodroplets[2] versus homogeneous nucleation and condensation of a gas into clusters, followed by ionization with an electron beam.[3] The atomization parameters can be adjusted to produce droplets with average diameters ranging from a few to hundreds of nanometers. Therefore these projectiles are typically larger than cluster ions.

Ion beam milling (IBM) is a subtractive manufacturing technique used to carve features with high aspect ratios. Based on physical sputtering, the etching rates of IBM are lowest among subtractive techniques because of its beam's low molecular flux,[4] which is limited by the space charge that develops between the plasma and accelerator screens. Maximum current densities produced by gridded, broad-beam ion sources typically range from 1–4 mA/cm^2.[5] Although faster subtractive techniques such as reactive ion etching are used for dry, anisotropic etching on many substrates of interest, inert materials such as SiC and B_4C offer great resistance to chemical attack, and for them, IBM with its slow rate is a competitive option. Furthermore, the slow rate of physical sputtering can be improved by replacing the small atomic ions of IBM with cluster ions[6] or in this case with charged nanodroplets. These massive projectiles have much lower charge to mass ratios, and significantly increase the beam molecular flux at the current densities capped by space charge.

This article presents measurements of the sputtering yield and sputtering rate of Si, SiC, and B_4C substrates bombarded by a beam of electrosprayed nanodroplets at normal incidence. Previously, Mahoney and co-workers[7,8] electrosprayed glycerol-based solutions in a vacuum to produce charged nanodroplets, and used them as projectiles for secondary ion mass spectrometry (SIMS). Like cluster ions, these large nanodroplets could desorb large macromolecules from both liquid and solid matrixes. Mahoney[9] also employed these energetic nanodroplets for surface cleaning. More recently, Hiraoka and co-workers[10,11] have resumed the research on electrosprayed nanodroplets as projectiles for SIMS. They atomize water-based solutions at atmospheric conditions, and introduce a fraction of the nanodroplets inside the vacuum chamber housing the analyte and a mass spectrometer. The article is organized as follows: after this introduction, Sec. II describes the experimental methodology and the characterization of the beams. Section III presents the sputtering results and a discussion of the findings. The article concludes with a brief summary.

II. EXPERIMENTAL APPARATUS AND METHODS

Beams of nanodroplets are produced by electrospraying in the cone-jet mode the ionic liquid 1-ethyl-3-methylimidazolium bis(trifluoromethylsulfonyl) imide (EMIIm).[12,13] The experimental setup is shown in Fig. 1. The electrospray source operates inside a vacuum chamber, and produces a conical beam of negatively charged droplets carrying a current I_E. The base pressure is 5×10^{-6} torr. The electrospray emitter is a platinum tube (0.16 mm inside diameter, 0.48 mm outside diameter) electrified at a potential V_E, typically −2130 V with respect to a facing extractor. A fraction of the electrospray escapes the emitter-extractor region through a small orifice (1.18 mm in diameter) drilled in the extractor, and coaxial with the emitter. The charge to mass ratio distribution $f(\xi)$, the mass flow rate $\dot{m}_B$, and the current I_B of the extracted beamlet are measured with a time-of-flight analyzer.[14] Alternatively, the beamlet is directed against a sputtering target at electric potential V_T. The accel-

[a]Author to whom correspondence should be addressed. Electronic mail: mgameroc@uci.edu.

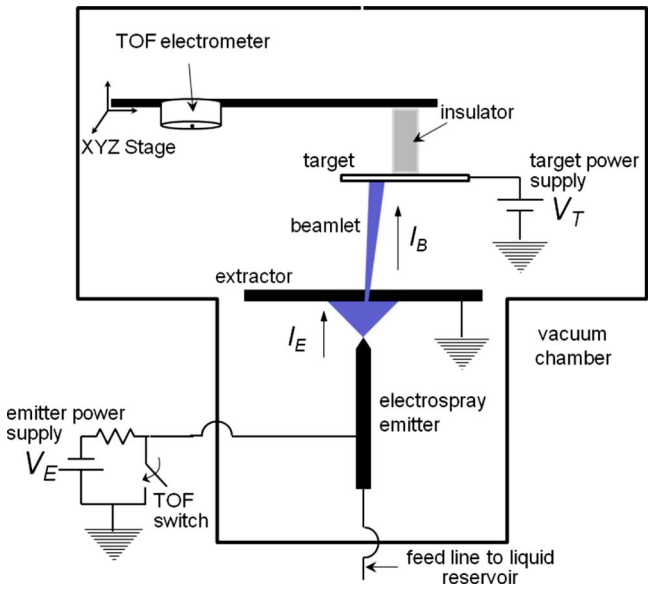

FIG. 1. (Color online) Experimental setup.

eration voltage of the beamlet is $V_A=V_T-V_E$. The velocity of a nanodroplet is $v_d=\sqrt{2\xi V_A}$. The kinetic energy of an EMIIm molecule is $E_m=m_m v_d^2/2=m_m \xi V_A$, where m_m is the molecular mass 391.12 amu. The pressure at the point of impact is of the order of $P=\rho v_d^2=2\rho\xi V_A$, where ρ is the liquid density, 1520 kg/m^3. The electrospray current I_E is proportional to the square root of the liquid flow rate, which is a controllable parameter.[15] The diameter and charge to mass ratio distributions of the droplets are functions of the liquid flow rate, or equivalently of I_E. The lower the electrospray current, the smaller the average droplet diameter and the larger the average charge to mass ratio. In summary, the average diameter, nanodroplet velocity, and molecular energy can be adjusted by changing the liquid flow rate and the acceleration voltage. Table I contains relevant parameters of the beams used in this study. The sputtering data were obtained at acceleration voltages between 9.13 and 20.13 kV, and for two values of the electrospray current, I_E=373 and 253 nA. The average diameters of the nanodroplets were estimated using the measured charge to mass ratio, and a charge level of 68% of the Rayleigh limit,[16]

$$\langle D\rangle = 0.68^{2/3}(288\gamma\varepsilon_0/\rho^2\langle\xi\rangle^2)^{1/3}. \quad (1)$$

ε_0 is the permittivity of the vacuum, and γ the surface tension of the liquid, 0.0349 N/m. Average droplet velocities are in the 6.70–3.44 km/s range. The molecular energies and typical impact pressures associated with these two velocities are 91.2 eV, 68.3 GPa, 24.1 eV, and 18.0 GPa. The molecular energies are much larger than the bond energies of the pairs Si–Si, C–Si, and C–B (1.94, 3.01, and 3.24 eV), and therefore the nanodroplets have the potential to produce considerable damage to the crystalline substrates.

The sputtering yield is calculated with the formula

$$Y = \frac{m_m}{\dot{m}_B \tau}\frac{n_C \rho_C V}{m_C}, \quad (2)$$

where V is the volume of material removed from the substrate, τ is the time of exposure to the beamlet, ρ_C is the density of the crystal (2330, 3200, and 2520 kg/m^3 for Si, SiC, and B_4C), and m_C and n_C are the mass and number of atoms in a crystal cell (28.08 amu and 1 for Si, 40.10 amu and 2 for SiC, 55.25 amu and 5 for B_4C). The position of the carved surface is determined with a profilometer, and its integration yields V. The sputtering rate is defined as

$$R = \frac{V}{A\tau}. \quad (3)$$

The area A is the normal projection of the carved surface on the planar face of the substrate. The Si target is a 2-in., prime grade [100] wafer. The SiC and B_4C targets are 2-in. polycrystalline disks with purities better than 99.5%, and manufactured by Feldco International via hot pressing.

III. RESULTS AND DISCUSSION

Figs. 2–5 show photographs, profiles, and atomic force microscope images of Si, SiC, and B_4C substrates bombarded for 15 min. The line of sight of the microscope in all photographs is perpendicular to the surface, which is illuminated with polychromatic light at grazing angle. Fig. 2 is for the Si target, I_E=373 nA and V_A=14.1 kV. The center of the photograph shows a circular and bright area bombarded by the beamlet, and surrounded by iridescent rings. The brightness is due to the scattering of light by a rough surface, while the darkness of the outer corners is due to the lack of normal reflection from the polished wafer. The profilometer shows that the bombarded area is approximately 7 μm deep, and that the surrounding region rises above the original surface. The beamlet removes silicon from the central area, and a fraction deposits nearby to form a thin film. The thickness of the film decreases at increasing separation from the depression. The colorful rings are produced by the interference of rays of light reflected from both the top of the film and the

TABLE I. Relevant parameters of the two nanodroplet beams used in this study: electrospray current I_E, beamlet current I_B, beamlet mass flow rate $\dot{m}_B$, average droplet charge to mass ratio $\langle\xi\rangle$, diameter $\langle D\rangle$, number of molecules $\langle N_m\rangle$, velocity $\langle v_d\rangle$, molecular energy $\langle E_m\rangle$, and impact pressure P. The last three parameters are computed at the extreme values of the acceleration voltage, 20.13 and 9.13 kV.

I_E (nA)	I_B (nA)	$\dot{m}_B$ (kg/s)	$\langle\xi\rangle$ (C/kg)	$\langle D\rangle$ (nm)	$\langle N_m\rangle$	$\langle v_d\rangle$ (km/s)	$\langle E_m\rangle$ (eV)	P (GPa)
373	38.7	4.67×10^{-11}	650	34.8	51660	5.11	53.1	39.8
						3.44	24.1	18.0
253	42.1	3.22×10^{-11}	1116	24.3	17520	6.70	91.2	68.3
						4.51	41.4	31.0

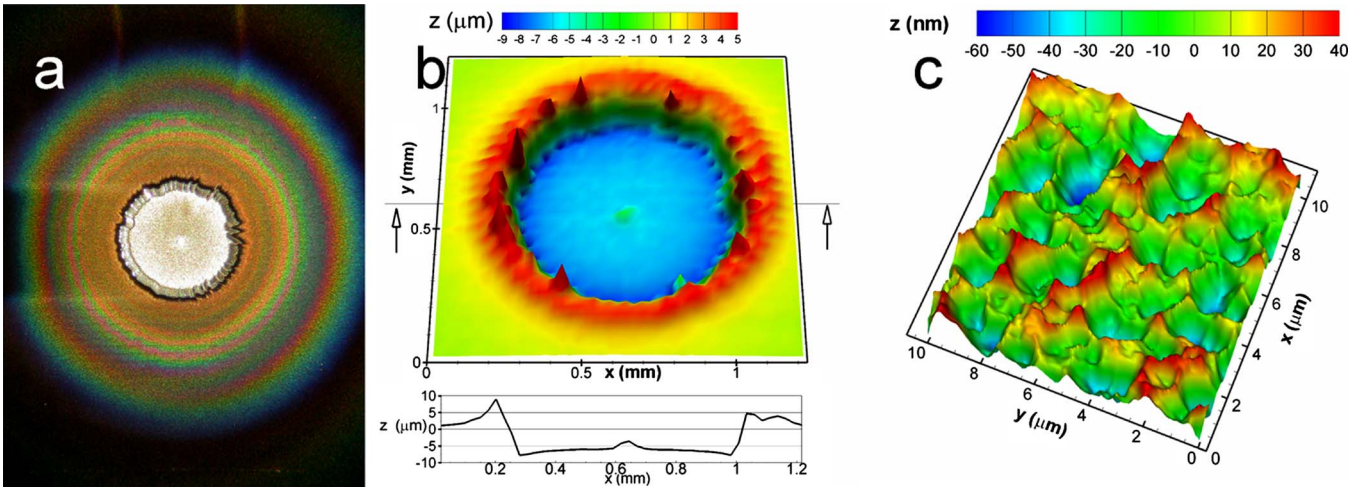

FIG. 2. (Color online) Photograph, profile, and AFM image of a Si target bombarded for 15 min with a beamlet of nanodroplets at 14.1 kV acceleration voltage, and 373 nA electrospray current (34.8 nm average droplet diameter, 4.28 km/s impact velocity, and 37.2 eV molecular kinetic energy).

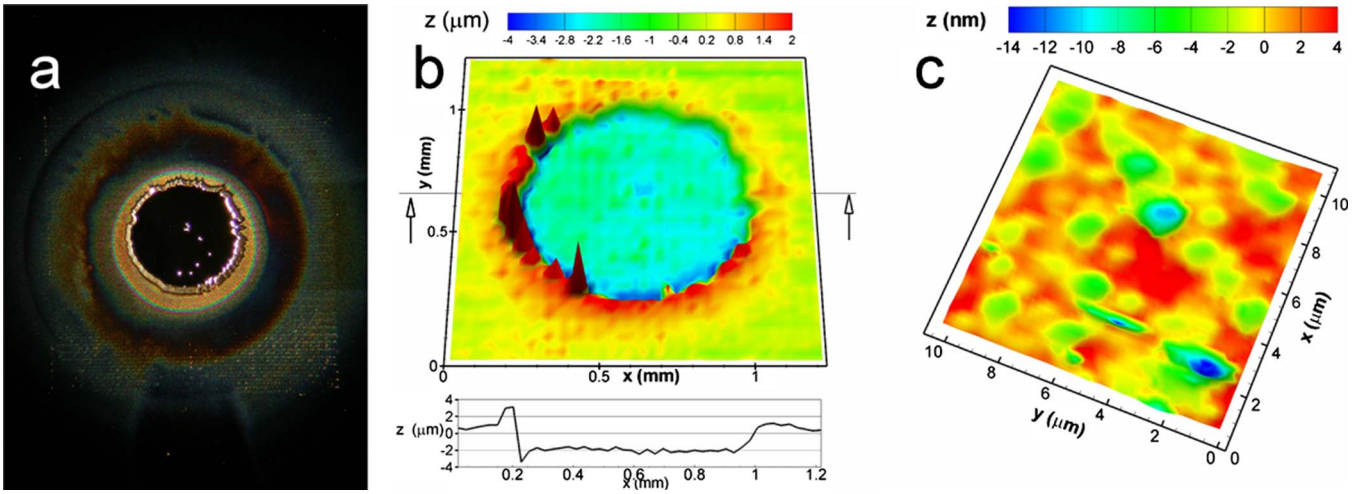

FIG. 3. (Color online) Photograph, profile, and AFM image of a Si target bombarded for 15 min with a beamlet of nanodroplets at 15.1 kV acceleration voltage, and 253 nA electrospray current (24.3 nm average droplet diameter, 5.81 km/s impact velocity, and 68.4 eV molecular kinetic energy).

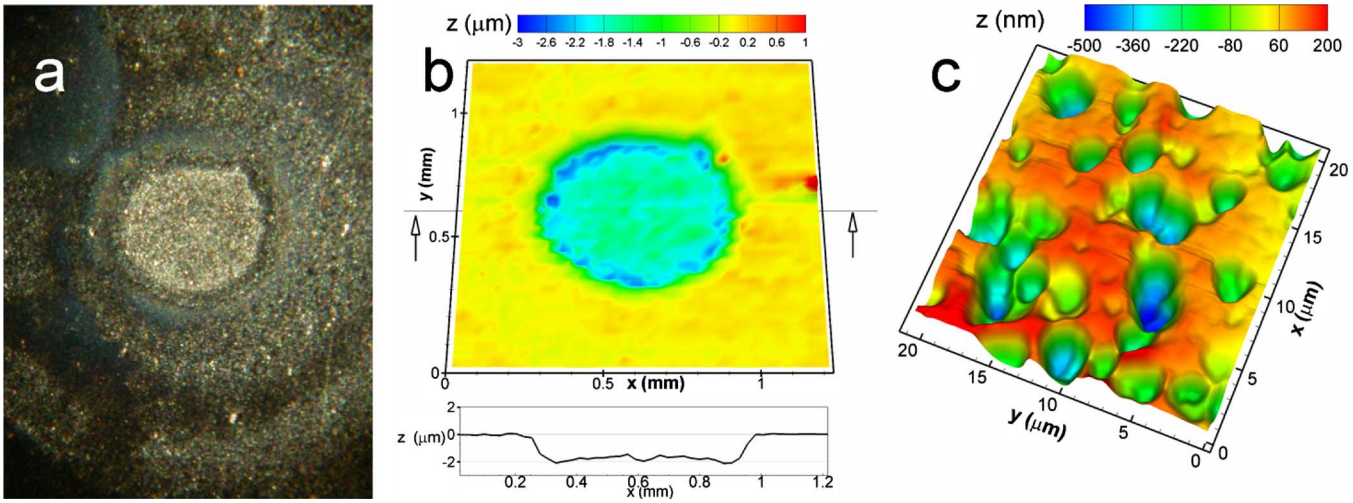

FIG. 4. (Color online) Photograph, profile, and AFM image of a SiC target bombarded for 15 min with a beamlet of nanodroplets at 18.1 kV acceleration voltage, and 253 nA electrospray current (24.3 nm average droplet diameter, 6.36 km/s impact velocity, and 82.0 eV molecular kinetic energy).

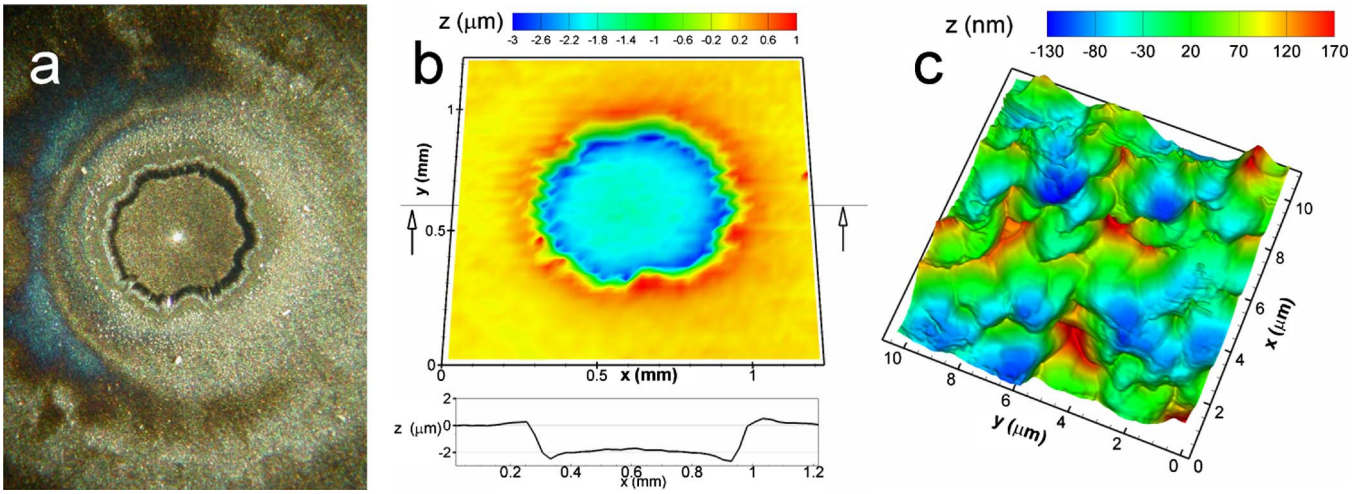

FIG. 5. (Color online) Photograph, profile, and AFM image of a B_4C target bombarded for 15 min with a beamlet of nanodroplets at 19.1 kV acceleration voltage, and 253 nA electrospray current (24.3 nm average droplet diameter, 6.53 km/s impact velocity, and 86.5 eV molecular kinetic energy).

surface of the wafer below, coupled with the monotonic decrease of the film thickness. The image recorded by atomic force microscopy (AFM) shows that the carved surface is made of a multitude of intertwined craters with diameters of a few micrometers, and depths of a few tens of nanometers. The rms roughness is 19.4 nm. These micron-sized features are responsible for the strong scattering of light and brightness of the depression.

Fig. 3 is for the Si target, I_E=253 nA and V_A =15.1 kV. The depression carved by the beamlet is approximately 2 μm deep, and has a specular surface. The rms roughness of the surface in Fig. 3(c) is 2.9 nm. The volumes of both ejected silicon and deposits surrounding the depression are smaller than in Fig. 2.

Fig. 4 is for the SiC target, I_E=253 nA and V_A =18.1 kV. The AFM image shows that the surface contains isolated micron-sized craters, surrounded by a smoother surface. The rms roughness is 160 nm. The depth of the depression is approximately 2 μm. There is no redeposition of sputtered material around the depression.

Fig. 5 is for the B_4C target, I_E=253 nA and V_A =19.1 kV. Similarly to the first Si target, the surface is made of superimposed micron-sized craters. The rms roughness of the surface in Fig. 5(c) is 63 nm. The depth of the depression is approximately 2 μm. There is a slight redeposition of sputtered material surrounding the depression.

Fig. 6 plots the sputtering yield of Si, SiC, and B_4C as a function of the molecular energy and for the two electrospray currents. The values of the acceleration voltages are given in auxiliary axes. Silicon has the highest yields, especially when the damaged surface is covered by micron-sized craters. We have observed that, depending on the acceleration voltage and the electrospray current, the bombarded Si surface is either smooth (see Fig. 3), or formed by micron-sized craters (see Fig. 2). For a given electrospray current, i.e., at fixed average droplet diameter and charge to mass ratio, the beam starts damaging the surface at relatively low voltages (typically 7 kV), the sputtering yield increases with the acceleration voltage, and micron-sized craters dominate the sputtered surface. When the acceleration voltage surpasses a critical value, which depends on the average diameter and charge to mass ratio of the droplets, the craters disappear and a smooth surface is carved. At this point the sputtering yield drops significantly. The smaller the droplets, the lower the acceleration voltage associated with the transition between the rough and specular surfaces. For example, the transition occurs around V_A=15 kV for I_E=373 nA, and near V_A =10 kV for I_E=253 nA. The sputtered surfaces of SiC and B_4C always contain micron-sized craters, at least within the range of acceleration potentials studied in this article. In the crater-sputtering mode the yield appears to be an increasing function of the molecular energy: beams with different average droplet diameters and acceleration voltages but equal molecular energy have similar sputtering yields. The maximum sputtering yields in Fig. 6 are 2.32, 1.48, and 2.29 atoms per molecule for Si, SiC, and B_4C; the energies of the EMIIm molecules are 37.3, 68.7, and 91.2 eV, respectively.

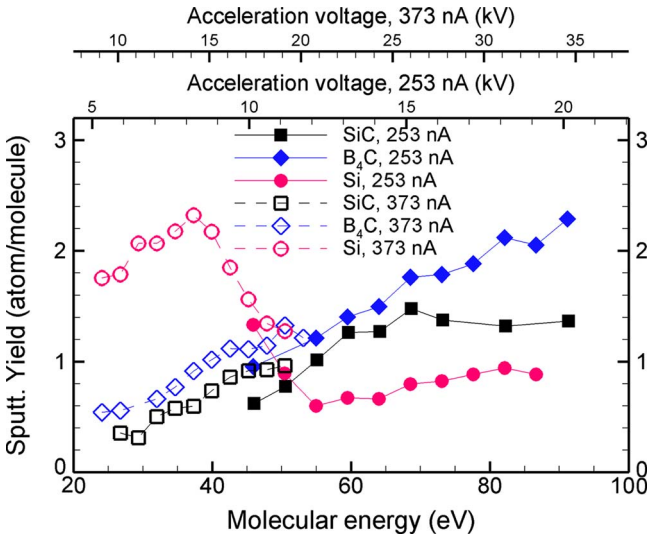

FIG. 6. (Color online) Sputtering yield (ejected atoms per EMIIm molecule) of Si, SiC, and B_4C as a function of the average kinetic energy of the EMIIm molecule, and for two electrospray currents (253 and 373 nA).

The sputtering yields of Si, SiC, and B_4C bombarded by argon at normal incidence and 500 eV are 0.4,[17] 0.8,[18] and 0.2 atoms per ion.[19]

An accurate determination of the threshold voltage for sputtering is not possible in our setup. A beamlet carries nanodroplets with different molecular energies because of the broad distribution of charge to mass ratio existing at any electrospray current. This variance of energies is especially problematic at the low acceleration voltages that start causing surface damage (typically 7 kV). Some droplets are energetic enough to sputter, while others cannot and form a layer of liquid on the surface. We have observed that this liquid deposit prevents the sputtering by the more energetic droplets.

We do not know whether the Im^- anions and EMI^+ cations making up the projectiles fragment into atoms upon impact. These are stable molecules with strong covalent bonds.[20] Previous work by Mahoney and co-workers[7,8] using glycerol nanodroplets with impact velocities comparable to ours does not show fragmentation of glycerol molecules. It is worth noting that the velocity and impact pressure of these nanodroplets are typical of hypervelocity impact, and that both types of collisions can produce craters many times larger than the size of the projectiles.[21] The field of hypervelocity impact deals with macroprojectiles, and length scales for which the solid target can be treated as a continuum with macro strain-stress properties. However, at the scale of a nanodroplet, a material such as monocrystalline silicon has very few dislocations, its strain-stress relation nears that of a perfect crystal, and the carving of a crater orders of magnitude larger than the projectile seems unfeasible. In fact, we have observed in silicon targets that micron-sized craters are formed only after an initial exposure time of approximately three minutes. Before this, shallow indentations of the order of the droplet size are formed. We think that most nanodroplets eject a volume of silicon comparable to its own, and at the same time create defects on the crystalline structure. The accumulation of defects would weaken the surface, and make it possible for impacts to occasionally produce micron-sized craters.

Fig. 7 shows the sputtering rate as a function of the acceleration voltage. The sputtering rate increases with V_A faster than the yield because the beamlets become narrower at increasing acceleration voltage, and therefore carve smaller areas [see Eq. (3)]. The maximum sputtering rates for Si, SiC, and B_4C are 448, 172, and 170 nm/min. The associated current densities at the target are 9.26×10^{-3}, 1.55×10^{-2}, and 1.33×10^{-2} mA/cm^2, respectively. It is worth comparing these values with those of gridded, broad-beam ion sources. A typical broad-beam ion source operates with argon at a current density of 2 mA/cm^2 and 500 V acceleration voltage. The space charge that forms between the plasma and the extraction grids imposes a fundamental limit on the current density and thus on the projectile flux, while energy values of the order of 1000 eV and larger cause ion implantation and undesired surface damage. Under these conditions a gridded ion source has sputtering rates of 60, 62, and 11 nm/min for Si, SiC, and B_4C, which are significantly smaller than those of nanodroplets. Furthermore, the current densities and sputtering rates of nanodroplet beams could be made much larger than the values in this article if a micromachined electrospray source with densely packed emitters were employed.[22]

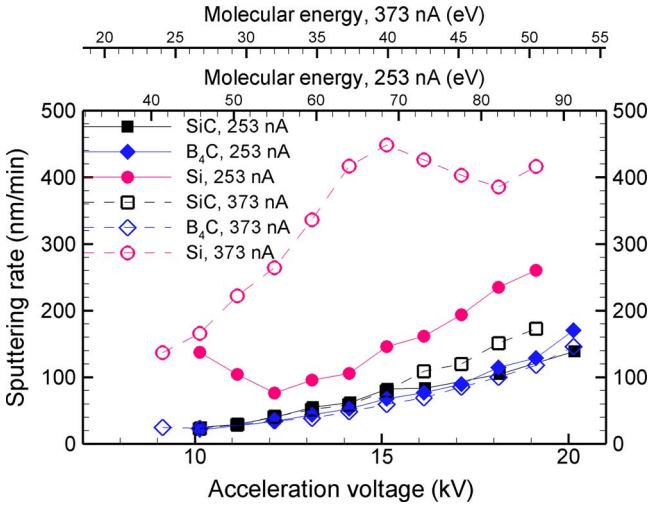

FIG. 7. (Color online) Sputtering rate (speed at which the substrate is carved) of Si, SiC, and B_4C as a function of the acceleration voltage, and for two electrospray currents (253 and 373 nA).

The use of the term sputtering to describe the ejection of material by energetic nanodroplets may require a justification. Traditionally, sputtering refers to the removal of surface atoms by the mechanism of cascade collisions, induced by energetic ions penetrating the surface.[23] More recently, larger projectiles such as cluster ions have been used to alter surfaces. Cluster ions with diameters of a few nanometers carve craters several times their size, do not necessarily penetrate into the substrate, and thermalization as well as cascade collisions processes play roles in the emission.[24] Despite these differences, the surface damage caused by cluster ions is commonly referred to as sputtering. Electrosprayed nanodroplets overlap with and extend the size range of cluster ions, and therefore we think that the use of the same label for these energetic projectiles is appropriate.

IV. CONCLUSION

The maximum sputtering yields of Si, SiC, and B_4C bombarded by electrospray nanodroplets are larger than one. These yields, combined with the high molecular flux of a single electrospray source, produce sputtering rates as high as 448, 172, and 170 nm/min, respectively. Depending on the substrate material, the size of the nanodroplets and the acceleration potential, the features carved on the surface vary from shallow indentations comparable to the size of the nanodroplets, to micron-sized craters. Thus, the rms roughness of the bombarded surface ranges from a few to hundreds of nanometers, resulting in the formation of both specular and diffusive surfaces. We plan to conduct additional research to unravel the mechanisms behind this novel nanodroplet/substrate interaction, and to investigate potential manufacturing applications.

[1]M. Gamero-Castaño and M. Mahadevan, Appl. Surf. Sci. **255**, 8556 (2009).
[2]J. Fernández de la Mora, Annu. Rev. Fluid Mech. **39**, 217 (2007).
[3]I. Yamada, J. Matsuo, and N. Toyoda, Nucl. Instrum. Methods Phys. Res. B **206**, 820 (2003).
[4]M. J. Madou, *Fundamentals of Microfabrication*, 2nd ed. (CRC, Boca Raton, 2002), Chap. 2.
[5]H. R. Kaufman and R. S. Robinson, in *Handbook of Ion Beam Processing Technology*, edited by J. J. Cuomo, S. M. Rossnagel, and H. R. Kaufman (Noyes Publications, Park Ridge, 1989), Chap. 2.
[6]I. Yamada, Nucl. Instrum. Methods Phys. Res. B **148**, 1 (1999).
[7]J. F. Mahoney, J. Perel, S. A. Ruatta, P. A. Martino, S. Husain, and T. D. Lee, Rapid Commun. Mass Spectrom. **5**, 441 (1991).
[8]D. S. Cornett, T. D. Lee, J. F. Mahoney, and P. J. Todd, Rapid Commun. Mass Spectrom. **8**, 996 (1994).
[9]J. F. Mahoney, Int. J. Mass Spectrom. Ion Process. **174**, 253 (1998).
[10]K. Hiraoka, K. Mori, and D. Asakawa, J. Mass Spectrom. **41**, 894 (2006).
[11]Y. Sakai, Y. Iijima, K. Mori, and K. Hiraoka, Surf. Interface Anal. **40**, 1716 (2008).
[12]A. B. McEwen, H. L. Ngo, K. LeCompte, and J. L. Goldman, J. Electrochem. Soc. **146**, 1687 (1999).
[13]M. Gamero-Castaño, Phys. Fluids **20**, 032103 (2008).
[14]M. Gamero-Castaño, J. Propul. Power **20**, 736 (2004).
[15]J. Fernández de la Mora and I. G. Loscertales, J. Fluid Mech. **260**, 155 (1994).
[16]M. Gamero-Castaño, Rev. Sci. Instrum. **80**, 053301 (2009).
[17]Y. Yamamura and H. Tawara, At. Data Nucl. Data Tables **62**, 149 (1996).
[18]T. S. Pugacheva, F. G. Jurabekova, Y. Miyagawa, and S. K. Valiev, Nucl. Instrum. Methods Phys. Res. B **127–128**, 260 (1997).
[19]T. Ono, T. Kawamura, K. Ishii, and Y. Yamamura, J. Nucl. Mater. **232**, 52 (1996).
[20]J. L. Goldman and A. B. McEwen, Electrochem. Solid-State Lett. **2**, 501 (1999).
[21]L. Davison, *Fundamentals of Shock Wave Propagation in Solids* (Springer-Verlag, Berlin, 2008).
[22]L. F. Velásquez-García, A. I. Akinwande, and M. Martínez-Sánchez, J. Microelectromech. Syst. **15**, 1272 (2006).
[23]P. Sigmund, Phys. Rev. **184**, 383 (1969).
[24]T. Aoki, T. Seki, and S. Ninomiya, Appl. Surf. Sci. **255**, 944 (2008).